The Influence of the Cell Geometry on the Signal Shape in Electron Drift Velocity Measurements*

A. F. Borghesani, L. Bruschi, M. Santini, and G. Torzo
Dipartimento di Fisica "G. Galilei", Università di Padova and Gruppo Nazionale Struttura della Materia, Padova

Z. Naturforsch. **41 a**, 912–920 (1986); received April 2, 1986

An accurate determination of the "time-of-flight" in swarm experiments with a parallel plate drift chamber requires that the time evolution of the charge induced on the collector is linear. This is obtained in very large chambers where the edge effects can be neglected. However, the experimental conditions of high-mobility carriers and highly pressurized gases impose some constraints on the acceptable drift cell dimensions. We have numerically calculated the effects of the finite size of the collector by exploiting the methods of the images. The numerical results have been experimentally checked using a suitable drift cell of variable geometry. As a result, a quantitative limit on the ratio between the collector radius and the drift distance has been established in order to design drift cells for which the edge effects can be neglected.

P.A.C.S. numbers: 2940, 4110 D, 3480 B

1. Introduction

One of the most common cell configuration for electron drift velocity measurements in swarm experiments is the "parallel-plate chamber". Here, two flat, parallel and, usually, circular electrodes are spaced by a known distance, d. A constant voltage is applied to the electrodes. Electrons injected into the drift space drift through the filling gas under the influence of the electric field from the negative electrode (the emitter) to the positive one (the collector). This is usually kept at a potential close to ground potential and the measuring apparatus is connected to it. If the density of the injected electrons is small enough to neglect space-charge effects and if the electrons are released far enough from the electrodes boundaries so that they move in a very uniform field, it can be assumed that the electrons drift at constant speed. The induced current flowing in the external circuit or the charge induced on the collector can be calculated either by applying the energy conservation principle [1–4] or by applying Green's reciprocation theorem [5–9].

In the first case, the induced current is given by

$$I = q\,(E/V_0)\,v\,, \tag{1}$$

where q is the moving charge, E is the electric field acting upon the charge, V_0 is the applied constant voltage and v is the drift velocity. E/V_0 depends only on the cell geometry and for parallel plate electrodes $E/V_0 = d^{-1}$, where d is the drift distance. So, I turns out to be a constant $= q/\tau$, where τ is the drift time or time-of-flight. By feeding the current I into a capacitor C, the voltage across it is simply given by

$$V(t) = \frac{1}{C}\int_0^t I(t')\,\mathrm{d}t' = \frac{q}{C}\frac{t}{\tau}\,. \tag{2}$$

For negative charges, $V(t)$ decreases linearly with time until the whole injected charge is collected.

In the second case, Green's reciprocation theorem immediately gives the total induced charge on the collector, which for the parallel plate configuration turns out to be directly proportional to the moving charge distance from the emitter:

$$Q_c = -\,q\,(1 - x/d)\,, \tag{3}$$

where x is the distance of the charge from the collector. So, if the charge drifts at constant speed, the current drawn from the external circuit to build up the necessary charge on the electrodes is constant, too. Also in this case the voltage drop across the measuring capacitor turns out to be a linear function of time. In either way, the transit time of the electron swarm can be accurately determined from an extrapolation of the linearly changing

* Work supported by Consiglio Nazionale delle Ricerche and Ministero Pubblica Istruzione, Rome, Italy. Reprint requests to: Dr. A. F. Borghesani, Dipartimento di Fisica, Università di Padova, Via F. Marzolo, 8, I-35131-Padova.

0340-4811 / 86 / 0700-0912 $ 01.30/0.

voltage waveform to find the start and end points of the electron motion in the drift space [10].

Both aforementioned methods are based on the assumption of field uniformity and on the understood hypothesis that the electric flux originating in the moving charge is completely linked with the electrodes. In fact, only in this case the total induced charge on the electrodes does equal the absolute value of the inducing charge, and the induced charge evolution on the collector follows a linear time dependence. However, there is not yet any quantitative suggestion on how far apart and how large with respect to their distance the electrodes have to be in order to satisfy the previously cited assumptions. It is normally accepted that they must be as large as possible to obtain a good field uniformity and that the addition of a guard ring, kept at about the same potential as the collector and closely surrounding it, greatly improves this uniformity [11]. Unfortunately, it is not always possible to make a cell following these criteria, particularly if the experiments are made with high-mobility electrons in highly pressurized gases. An accurate measurement of the drift time requires then a large drift distance, while a maximum electrode radius cannot be exceeded in order to avoid large mechanical stresses on the cell walls. In this situation, it may happen that the electrons released from the emitter are not far enough from the collector boundaries, so that a finite fraction of the electric flux is linked with the guard ring and $V(t)$ differs from a straight line. A good determination of the drift time is, however, still possible if the finite duration of the electron injection and the electron diffusion and attachment processes can be neglected. In fact, under such assumptions the beginning and the end of the voltage waveform are sharply defined. Unfortunately, these effects round off the edges of the voltage ramp and therefore the drift time must be determined by the previously outlined procedure with an accuracy which gets worse as the curvature of $V(t)$ grows larger.

Clearly, one expects that the deviations from linearity become larger as the collector radius becomes smaller, but up to now there are no quantitative evaluations of these effects. There are only calculations to ascertain the edge effects on the charge induced on the collector of a semi-infinite parallel plate chamber when the inducing charge is released near the straight, indefinitely long boundary line [4]. We have therefore performed numerical calculations to predict the shape of the voltage signal for different values of R/d, where R is the collector radius. To compare these calculations with the experiment, we have constructed and operated a simple parallel plate cylindrical drift cell in which the collector radius and the drift distance can be easily varied. The experimental and numerical results agree very well, thus allowing us to give a quantitative lower limit for the ratio R/d which makes the edge effects negligible.

In Sect. 2 the experimental cell and the electrical circuitry are described; in Sect. 3 the mathematical problem to calculate the instantaneous induced charge on a finite size collector is set out and the numerical calculation details are exposed. In Sect. 4 the numerical and experimental results are quoted and compared. Finally, in Sect. 5 the conclusions are drawn.

2. The Experimental Apparatus and Procedure

The experimental cell and the measuring electronics are depicted in Figure 1.

The two gold-coated brass electrodes are contained in a cylindrical brass cell. The upper electrode has a diameter of 75 mm and it is suspended from the upper flange by means of four PVC spacers. The central portion of this electrode has a seat for an UV-grade fused silica disk (2.5 cm diameter, 1 mm thickness) with the lower face coated with a 200 Å thick Au film. The silica disk is pressed onto the electrode by a Viton O-ring to provide a good electrical contact for the gold film. A circular window (4 mm diameter) in the seat allows electrons to be emitted from the gold film when it is irradiated from the back with UV light by a pulsed low power Xenon flash lamp (EG & G, model 108FXAU) through the UV-grade fused silica window embedded in the upper cell flange. The light pulse lasts $\approx 9\,\mu s$. Details on the properties and performance of such an emitter have been already described elsewhere [12].

The lower electrode is a multiple-collector assembly. It rests on a PVC supporting disk and it consists of a central circular electrode with a diameter of 8 mm, coaxial with the electron emitting area of the upper electrode and surrounded by five concentric rings of increasing diameters. The

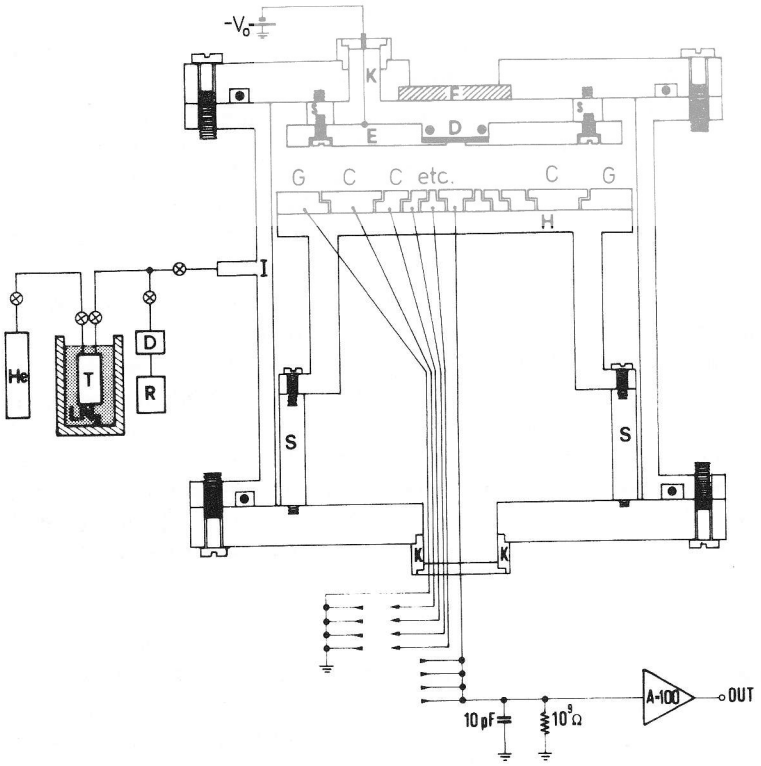

Fig. 1. Schematic drawing of the apparatus. The drift cell is drawn to scale, while the remaining parts are not. Meaning of the lettering: K = electrical feedthroughs, S = PVC spacers, F = fused silica window, D = gold-coated fused silica disk, E = emitting electrode, C = variable-radius collecting electrode, H = PVC collector support, G = guard ring, I = gas inlet, T = liquid N_2 cooled active charcoal trap, D = diffusion pump, R = roughing pump, He = Helium flask.

outer diameters of these concentric electrodes are 12, 20, 32, 60 and 80 mm, respectively. The radius of the innermost electrode is twice as large as the radius of the electron emitting area. The latter has been so chosen as to have a good compromise between two opposing requirements: a transversally narrow charge injection in order to minimize the influence of the lateral diffusion and a reasonably large amount of injected electrons in order to have an easily detectable signal.

The gap between two consecutive annuli is about 0.5 mm. These electrodes are so shaped as to completely screen the insulating support. The central electrode is connected to the measuring electronics. Each of the remaining electrodes may be either shunted to ground or connected to the central electrode. By properly connecting them it is then possible to change the effective collector radius without opening the cell. The outermost electrode and the cell walls are always grounded.

The drift distance can be varied by adding suitable spacers under the support. In our measurements we have chosen two drift distances of 10 and 20 mm, thus obtaining the following R/d values set: 0.2, 0.3, 0.4, 0.5, 0.6, 0.8, 1.0, 1.5, 1.6, and 3.0.

The current pulse is integrated by a 10 pF capacitor in parallel with the cell capacitance and with the stray wires capacitance so that the effective integration capacitance C_E depends on how the ring electrodes are connected and on how large the drift distance is. The value of C_E has been determined for each electrode connection and drift distance by operating the drift cell under vacuum and measuring the time evolution of the capacitor discharge through the $10^9\,\Omega$-resistor. The measured time constants ranged between 25 and 60 ms corresponding to $25\text{ pF} < C_E < 60\text{ pF}$. The integration time constants are chosen much larger than the electron time-of-flight (in our case $\approx 10-20\,\mu s$), resulting in a large signal-to-noise ratio and a low signal distortion.

The voltage signal across the capacitor is then fed to a non-inverting amplifier with a gain of 100 (LF357). The amplifier output is recorded by a storage oscilloscope (HITACHI, model VC6041) and plotted by an X−Y recorder.

The filling gas, 99.9996% ultra pure He at a pressure of ≈ 0.30 MPa was passed through an active charcoal trap cooled at 77.4 K before entering the cell. This was flushed with the gas many times before making the measurements. For each elec-

trodes connection, measurements were made at several voltages to ascertain the influence of the attachment and diffusion processes. At the end of the measurement cycle, the measurements with the largest electrode were repeated to check whether the impurity content did significantly change, but no noticeable effect was detected.

3. Numerical Calculation of the Induced Charge

We want to calculate the time evolution of the charges induced on the conducting plates of an infinite parallel plate capacitor by a point charge drifting therein. If the applied electric field is constant, the method of the images is well suited because, for time varying signals, the plates can both be assumed to be grounded.

A straightforward application of this method (see Fig. 2) leads to an infinite set of images of alternating signs and alternating spacings [13–15]. Many mathematical techniques have been devised to evaluate the sum of the conditionally convergent infinite series for the infinite capacitor [16–19]. In

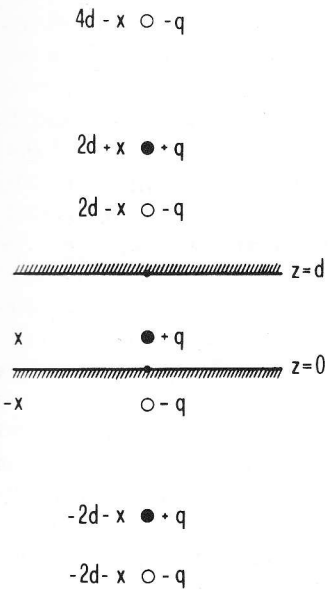

Fig. 2. The infinite series of image charges generated on the two conducting infinite surfaces located at $z = 0$ and $z = d$ by repeated reflection of a point charge q located at $z = x$. The z-axis is taken along the line of the image charges. Closed symbols represent image charges of the same polarity as the inducing one. Open symbols refer to opposite polarity charges.

any case, the solution for the total charge induced on the collector is obviously the same as the one obtained by applying Green's reciprocation theorem (3).

In our case, however, we will directly deal with the infinite series which give the charge distribution and the total induced charge.

Let us consider two infinite circular conducting plates with a circular cylindrical coordinate system fixed on the collector. The z-axis is the cylindrical symmetry axis of this configuration. It is convenient to introduce primed dimensionless variables by scaling distances, times, and charges by the appropriate relevant parameters, d = drift space, τ = drift time, and q = drifting charge. Thus, the plates ar separated by a distance $d' = 1$. The collecting plate is at $z' = 0$ and the emitting one is at $z' = 1$. A point on the collector has the coordinates $(r', \varphi, 0)$, where φ is the azimuthal angle. Let us consider only the charge induced on a central circular collector portion of radius $R' = R/d$, insulated from the rest of the plate, which thus acts as a guard ring. Let us then suppose that a unit point charge, $q' = 1$, is moving at constant speed towards the collector along the symmetry axis. At time $t' = 0$ the charge starts drifting at $z' = 1$ and at time $t' = 1$ it arrives at $z' = 0$. When the charge is at $z' = x'$ at time t', the surface charge density, σ', on the collector can be easily computed (see Fig. 2) and it is given by [9, 19]

$$\sigma'(r', t') = \frac{1}{2\pi} \sum_{m=1}^{\infty} \left\{ \frac{2m - x'}{[(2m - x')^2 + r'^2]^{3/2}} - \frac{2(m-1) + x'}{\{[2(m-1) + x']^2 + r'^2\}^{3/2}} \right\}. \tag{4}$$

The total charge induced on the central disk of radius R' is simply given by

$$Q'(t', R') = 2\pi \int_0^{R'} r' \sigma'(r', t')\, dr'$$

$$= \sum_{m=1}^{\infty} \left\{ \frac{2(m-1) + x'}{\{[2(m-1) + x']^2 + R'^2\}^{1/2}} - \frac{2m - x'}{[(2m - x')^2 + R'^2]^{1/2}} \right\}. \tag{5}$$

Both σ' and Q' depend on t' through $x' = 1 - t'$.

There are three interesting limits for $Q'(t', R')$, which must be considered in order to check the

numerical results:

$$\lim_{t' \to 0} Q'(t', R') = 0 , \tag{6.a}$$

$$\lim_{t' \to 1} Q'(t', R') = -1 , \tag{6.b}$$

$$\lim_{R' \to \infty} Q'(t', R') = 2\pi \int_0^\infty r' \sigma'(r', t')\, dr' = -(1 - x') ,$$

$$\text{for} \quad 0 \leqq x' \leqq 1 . \tag{6.c}$$

The first limit means that the electric flux is completely linked with the emitter as the charge gets started. The second one tells us that in absence of diffusion and attachment processes the whole drifting charge reaches the collector. Finally, the third limit means that the Green's reciprocation theorem solution has to be recovered by the numerical calculations relying on the images method for an infinite collector.

Up until now, we have assumed an instantaneous charge injection and we have neglected the attachment and diffusion processes. This is not the experimental case, however. The light pulse of the Xenon flash lamp has in fact a finite duration ($t_0 \approx 9\,\mu s$), so that the electron injection cannot be approximated at all by a δ function. However, if the electron injection has a time dependence expressed by a function $N(t')$, the total induced charge on the collector at time t' is given by the time convolution of $N(t')$ with $Q'(t', R')$:

$$Q'_I(t', R') = \int_0^{t'} Q'[(t' - \omega), R']\, N(\omega)\, d\omega ,$$

$$\text{for} \quad t' \leqq 1 . \tag{7}$$

Equation (7) gives also the charge stored in the measuring capacitor Q'_C. For $t' > 1$ the induced charges are neutralized step by step by the incoming charge, while an equal amount of charge is being stored in the capacitor. So, for $t' > 1$ we have two equations for the induced charge Q'_I and for the stored charge Q'_C:

$$Q'_I = N(t' - 1)\, Q'(1, R') + \int_{t'-1}^{t'} N(\omega)\, Q'[(t' - \omega), R']\, d\omega \tag{8}$$

and

$$Q'_C = Q'(1, R') \int_0^{t'-1} N(\omega)\, d\omega + \int_{t'-1}^{t'} N(\omega)\, Q'[(t' - \omega), R']\, d\omega , \tag{9}$$

Only Q'_C is directly measurable, and from now on we will focus our attention on it. The function $N(t')$ can be obtained by measuring the output signal in vacuo with a small integration constant [12]. Its form has been interpolated by mean of the cubic splines method [20] and it is therefore numerically available, so that the convolution integral can readily be approximated by a summation.

Furthermore, in real experiments the electron diffusion and attachment processes may not be neglected. In the mathematical scheme of the method of the images the electron diffusion process is not easy to be treated, for it leads to complicated elliptical integrals. But this effect can be made small by performing measurements with sufficiently high electric fields and with small electron emitting areas, and therefore it has not been presently taken into account. On the contrary, the attachment process is very easy to be accounted for by the images method scheme because the attached electrons can be assumed to remain fixed on the symmetry axis. (Negative O_2 ions have indeed a mobility ≈ 1000 times smaller than that of the free electrons.) Under these assumptions, the numerical procedure to get the instantaneous total induced charge is the following.

First of all, the drift time was discretized by dividing it into 50 subintervals placing there 51 equally spaced nodes t'_i, where $t'_1 = 0$ and $t'_{51} = 1$. Then $Q'(t'_i, R')$ was computed for each R' and t'_i through (5) by evaluating directly the sum of the series and also by numerically performing the integration by exploiting an adaptative quadrature routine [21] based on Simpson's integration rule as a check. The upper ∞ limit of the summation index was replaced by 200. This is justified because $\sigma'(r', t')$ and $Q'(t', R')$ converge uniformly in r' [19] (Weierstrass M test [22]) and the truncation error turns out to be completely negligible for our purposes. The computed $Q'(t'_i, R')$ values satisfy conditions (6.a) and (6.b), while condition (6.c) is satisfied for $R' \geqq 2.5$ with great accuracy (well within 0.2%). The $Q'(t'_i, R')$ values have then been interpolated with cubic splines to allow further, more refined calculations.

To evaluate the time convolution in (7), (8), and (9), also taking into account the attachment process we have further divided the drift time in $L = 100$ subintervals. The drift distance is also discretized in L subintervals of amplitude $h' = 1/L$. Let us then

define $M = L t'_0$, with $t'_0 = t_0/\tau$, as the number of time subintervals over which the light pulse $N_i = N(t'_i)$ has a non-zero value. Let us further define $L_1 = M + 1$, $L_2 = L + 1$, $L_3 = L_1 + L_2 - 1$. The attachment process is described by a fractional charge loss which depends exponentially on the distance travelled by the electrons. So, if λ' is the electron mean free path for this process, the moving charge is reduced by a factor $\alpha = \exp(-h'/\lambda')$ at each step, while a corresponding fraction $\beta = 1 - \alpha$ is left at the previous position as a static charge.

Injection gets started at $t' = t'_1$ and stops at $t' = t'_{L_1}$. The first injected charge arrives at the collector at $t' = t'_{L_2}$, and at time $t' = t'_{L_3}$ charge collection is completed. Let us furthermore define $Q'_i \equiv Q'(t'_i, R')$ and $Q'_C \equiv Q'_C(t', R')$. The function $N(t')$ has been normalized so that the total injected charge is unity:

$$\int_0^{t'_0} N(\omega)\, \mathrm{d}\omega = \sum_{m=1}^{L_1} N_m = 1 .$$

The charge stored in the capacitor is then given by the following equations:

$$Q'_C = \sum_{j=1}^{m} \alpha^{m-j} N_j Q'_{m-j+1} + \beta \sum_{j=1}^{m-1} \alpha^{m-j-1} Q'_{m-j} \sum_{k=1}^{j} N_k ,$$

$$\text{for} \quad 1 \leqq m \leqq L_1 , \qquad (10)$$

$$Q'_C = \sum_{j=1}^{L_1} \alpha^{m-j} N_j Q'_{m-j+1} + \beta \left\{ \sum_{j=1}^{M} \alpha^{m-j-1} Q'_{m-j} \sum_{k=1}^{j} N_k + \sum_{j=L_1}^{m-1} \alpha^{m-j-1} Q'_{m-j} \right\} ,$$

$$\text{for} \quad L_1 < m \leqq L_2 , \qquad (11)$$

$$Q'_C = \alpha^L Q'_{L_2} \sum_{j=1}^{m-L} N_j + \sum_{j=m-L+1}^{L_1} \alpha^{m-j} N_j Q'_{m-j+1} + \beta \left\{ \sum_{j=L_1}^{m-1} \alpha^{m-j-1} Q'_{m-j} + \sum_{j=m-L}^{M} \alpha^{m-j-1} Q'_{m-j} \sum_{k=1}^{j} N_k \right\} ,$$

$$\text{for} \quad L_2 < m \leqq L_3 . \qquad (12)$$

For $m \geqq L_3$, the final charge stored in the capacitor is

$$Q'^{*}_C \equiv Q'_C(t' \geqq 1 + t'_0, R') = \alpha^L Q'_{L_2} + \beta \sum_{j=1}^{L} \alpha^{j-1} Q'_j . \qquad (13)$$

The first term of the r.h.s. of (13) represents the contribution due to the charges which have effectively arrived at the collector. The second one is the contribution due to the static charges left behind in the drift space.

4. Comparison of the Experimental and Numerical Results

The records of the voltage signals obtained with an electric field $E = V_0/d = 30$ V/cm are reported in Fig. 3 for the R' values with $d = 1$ cm and in Fig. 4 for the R' values with $d = 2$ cm. The maximum voltage amplitude is different for each curve because it depends on the effective integration capacitance. However, the quantity $C_E V_{max}/e \approx 6 \times 10^5$ electrons is constant for each R' value. This means that the lateral diffusion process did not play a relevant role. This is consistent with the prediction of the maximum electron beam spreading $\langle (\Delta r)^2 \rangle^{1/2} \approx (2 k_B T d/e E)^{1/2}$, which in our measurements turns out to be of the order of 0.5 mm, much less than the difference between the diameters of the emitting area and of the smallest collecting electrode. Furthermore, no space-charge effects have been detected, because the signal shape did not change for a ≈ 10 times smaller electron injection obtained by decreasing the flash lamp intensity. The time-of-flight obtained in the measurements with a drift distance of 2 cm (i.e., for the sets $R' = 0.2$, 0.3, 0.5, 0.8, and 1.5) is not strictly twice as large as the one obtained with $d = 1$ cm, but it is $\approx 10\%$ larger. This difference is due to a $\approx 10\%$ pressure difference in the two runs.

The results of the numerical calculations ((10), (11), and (12)) are also reported in the figures. The calculations were performed introducing $\tau = 9.4\ \mu$s for $d = 1$ cm and $\tau = 20.5\ \mu$s for $d = 2$ cm. The parameter λ' has been estimated to be of the order of 10 for $d = 1$ cm and 5 for $d = 2$ cm, assuming an O_2 concentration of a few p.p.m. [23]. In any case, as long as λ' is greater than unity and once the curve has been normalized to the appropriate final value,

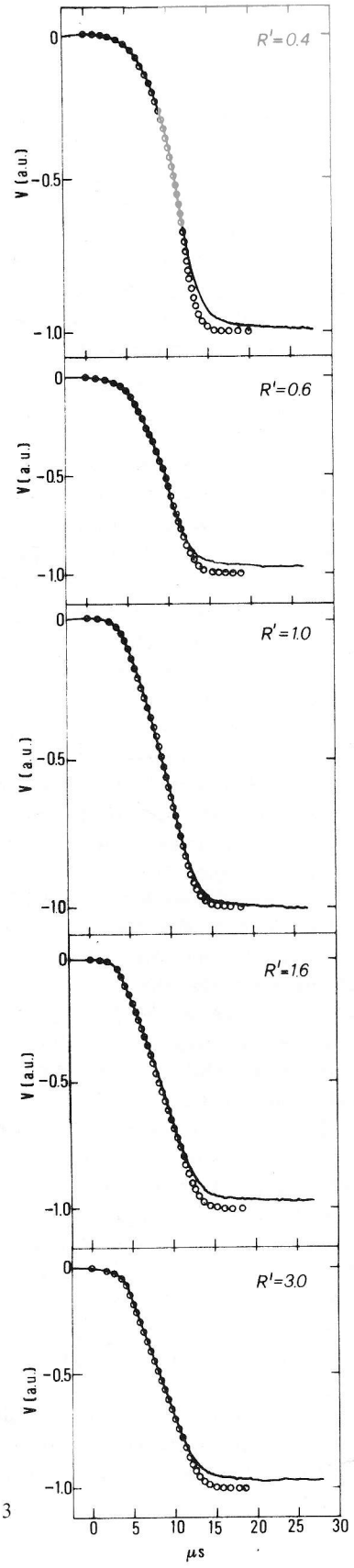

Fig. 3

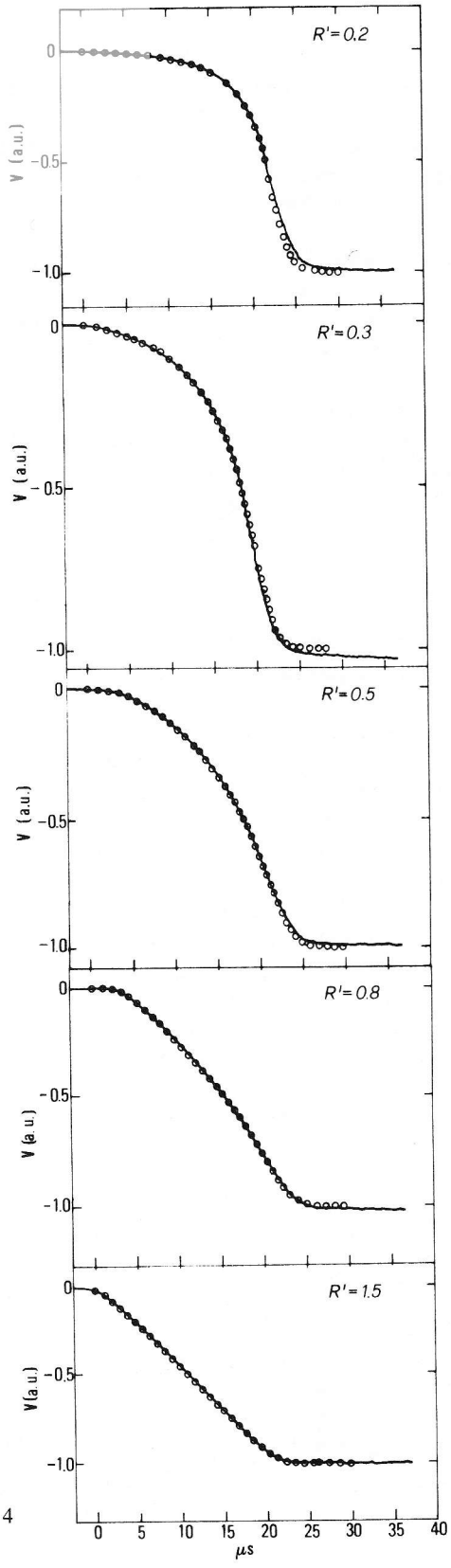

Fig. 4

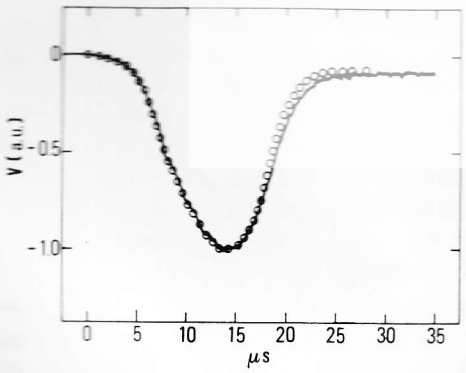

Fig. 5. Signal shape obtained by grounding the central portion of the collecting electrode and connecting the remaining electrodes to the measuring apparatus. Continuous curve: experimental recording obtained with a drift distance of 1 cm, an electric field of 25 V/cm, and a pressure of ≈ 0.30 MPa of Helium. Open circles: numerical results obtained with $\tau = 24.1$ μs, $t_0 \approx 9$ μs, and $\lambda' = 10$.

there is no a large distortion of the curve shape (well within a few percent) owing to the attachment process.

As it can be observed, there is an almost perfect agreement between the experimental and the computed curves. The little discrepancy between them is due to the neglected electron diffusion process that tends to smooth the final part of the experimental curve.

It has also to be noted that for $R' > 1.5$ the curves are practically straight lines (except at the ends, where the finite injection duration does strongly influence the signal shape). So, the ratio $R/d \approx 1.5$ can be assumed as the minimum value to construct a god parallel-plate drift chamber endowed with a guard ring.

It would also be interesting to see what happens on the guard ring when the charge is drifting towards the collector. One expects that charge is also induced on the guard ring in a way that depends on the solid angle under which the guard ring is seen by the drifting charge. So, the charge induced on the guard ring should increase until the drifting charge arrives at half the way from the collector and then decrease to zero when the charge is collected. To test this prediction the connection of the elctrodes has been modified by shunting to ground the central electrode and connecting the remaining ones to the measuring apparatus. The resulting signal obtained with an applied field $E = 25$ V/cm and a drift distance $d = 1$ cm is depicted in Figure 5. The signal can also be numerically predicted by subtracting the curve calculated for $R' = 0.4$ from that calculated for $R' = 3.0$ with $\tau = 24.1$ μs. The properly normalized computed curve is also shown in Figure 5. There is a nearly perfect agreement between the two curves.

Fig. 3. Signal shapes obtained with a drift distance of 1 cm, an electric field of 30 V/cm, and a pressure of ≈ 0.30 MPa of Helium for several R/d values. Continuous curves: experimental recordings. Open circles: numerical computation results obtained with $\tau = 9.4$ μs, $t_0 \approx 9$ μs, and $\lambda' = 10$. The size of the symbols is greater than the error bar associated with the choice of the mean free path for the attachment process, λ'.

Fig. 4. Signal shapes obtained with a drift distance of 2 cm, an electric field of 30 V/cm, and a pressure of ≈ 0.30 MPa of Helium. Continuously curves: experimental recordings. Open circles: numerical computation results obtained with $\tau = 20.5$ μs, $t_0 \approx 9$ μs, and $\lambda' = 5$.

5. Conclusions

When performing electron drift velocity measurements in parallel plate chambers, one is faced with the problem to extract the electron drift time from the time evolution of the charges induced on the collector. If one could work with an ideal indefinitely large cell, there were no problems: if the electrons drift at constant speed, the recorded signal has a linear time dependence and the drift time can be accurately determined.

However, this ideal situation does never occur in the actual experimental arrangements, where the drift cells have finite dimensions. So, one has to take into account the edge effects and to try to minimize them. To perform this job, it is necessary to know how the induced charges are distributed on the collector. Once the charge distribution is known, the total charge induced on collectors of different size can be computed and the waveform recorded during the electron motion can be numerically predicted. These numerical predictions have been experimentally confirmed by recording the signal shape obtained operating a drift cell of suitably variable geometry.

From our numerical and experimental results it can be also deduced that the ratio R/d of the cell configuration should be at least ≈ 2, in order to have almost perfectly linear signals from which the

electrons drift time can be accurately determined. For lower R/d values the finite size of the collector strongly affects the signal shape, even preventing any determination of the drift time. It is therefore necessary to design parallel plate drift chambers in such a way that that lower bound on R/d is satisfied.

One must, however, be aware of the great importance to have in any case a guard ring surrounding the collector and separating it enough from the lateral walls of the cell in which the electrodes are contained. In fact, in our calculations we have supposed such lateral walls to be at infinity, while in our experimental setup a guard ring with a minimum width of ≈ 10 mm was always in place. We can thus assume that the mutual influence between the charges induced on the lateral walls and those induced on the collecting electrode is efficiently screened by the presence of the guard ring. In this case the results we obtained turn out to be correct. In the opposite case, when no guard ring is present and the collector boundaries are near to the walls, one can get non linear curves even for R/d values higher than ≈ 2.

[1] J. J. Spokas, Amer. J. Phys. **46** (12), 1279 (1978).
[2] A. J. Walton, Amer. J. Phys. **45** (11), 1177 (1977).
[3] J. Sharpe and D. Taylor, Mesure et dètection des rayonnements nùclèaires, Dunod, Paris 1958, p. 219.
[4] B. B. Rossi and H. H. Staub, Ionization chambers and counters. Experimental techniques, McGraw-Hill, New York 1949, p. 20–55.
[5] W. Franzen and L. W. Cochran, Pulse ionization chambers and proportional counters, in: Nuclear instruments and their uses, A. H. Snell ed., J. Wiley & Sons, New York 1962, p. 3–81.
[6] W. R. Smythe, Static and dynamic electricity, McGraw-Hill, New York 1968, p. 35.
[7] J. S. Gordon and E. Mathieson, Nucl. Instrum. Meth. Phys. Res. **227,** 267 (1984).
[8] E. Mathieson and J. S. Gordon, Nucl. Instrum. Meth. Phys. Res. **227,** 282 (1984).
[9] E. Durand, Electrostatique: Problemes generaux conducteurs, Masson et C.ie, Paris 1966, p. 158 and 196–197.
[10] S. R. Hunter and L. G. Christophorou, Electron motion in low- and high pressure gases, in Electron molecule interactions and their application, Vol. II, L. G. Christophorou ed., Academic Press, New York 1984.
[11] A. K. Bartels, Ph. D. Thesis, Hamburg 1974.
[12] A. F. Borghesani, L. Bruschi, M. Santini, and G. Torzo, A simple photoelectronic source for swarm experiments in high density gases, to be published.
[13] E. Durand loc. cit. p. 200–201.
[14] J. H. Jeans, The mathematical theory of electricity and magnetism, Cambridge University Press, Cambridge 1915, p. 185.
[15] M. Zahn, Amer. J. Phys. **44** (11), 1132 (1976).
[16] B. G. Dick, Amer. J. Phys. **41,** 1290 (1973).
[17] J. J. G. Scanio, Amer. J. Phys. **41,** 415 (1973).
[18] R. G. Barrera, O. Guzmán, and B. Balaguer, Amer. J. Phys. **46** (11), 1172 (1978).
[19] W. A. Newcomb, Amer. J. Phys. **50** (7), 601 (1982).
[20] G. E. Forsythe, M. A. Malcolm, and C. B. Moler, Computer methods for mathematical computations, Prentice-Hall Inc., New York 1977, p. 76.
[21] L. F. Shampine and R. C. Allen Jr., Numerical computing: an introduction, W. B. Saunders Co., Philadelphia 1900, p. 67, 239, and ff.
[22] G. Arfken, Mathematical methods for physicists, Academic Press, New York 1985, p. 301.
[23] J. L. Pack and A. V. Phelps, Phys. Rev. **221,** 798 (1961).